Improving dike reliability estimates by incorporating construction survival

van der Krogt, Mark G.; Schweckendiek, Timo; Kok, Matthijs

DOI
10.1016/j.enggeo.2020.105937

Publication date
2021

Document Version
Final published version

Published in
Engineering Geology

Engineering Geology 280 (2021) 105937

Contents lists available at ScienceDirect

Engineering Geology

journal homepage: www.elsevier.com/locate/enggeo

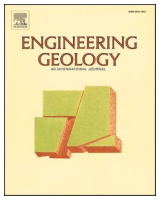

Improving dike reliability estimates by incorporating construction survival

Mark G. van der Krogt [a,b,*], Timo Schweckendiek [a,b], Matthijs Kok [a]

[a] Faculty of Civil Engineering and Geosciences, Delft University of Technology, Delft, The Netherlands
[b] Deltares, Delft, The Netherlands

ARTICLE INFO

Keywords:
Slope stability
Reliability analysis
Bayesian updating
Dike
Levee
Survival information

ABSTRACT

During construction of a dike, slope stability often reaches critical levels, due to the excess pore water pressures in the foundation. The loading condition during construction has similarities with the design conditions during flood loading. Not only in terms of the pore water pressures as the main driving force, but also in terms of criticality of the stability. This paper examines how the information of survival of the construction stage can be used to improve the reliability estimate for a dike in flood conditions, using Bayesian updating. The approach is exemplified for a range of typical dikes and for a case study of a full-scale test embankment. The main result is that the reliability can increase significantly by including the information of construction survival and the uncertainty reduction involved, especially for dikes on soft soil blankets. For the investigated cases, the posterior failure probability was up to several orders of magnitude lower than the prior failure probability. The main factors influencing the degree of reliability update, were the ground conditions and the degree of criticality of the slope stability during construction. In conclusion, using the information of the survived construction leads to improved reliability-based safety assessments of dikes, and consequently to more targeted and cost-effective flood protection.

1. Introduction

Dikes protect land from flooding, which is crucial for low-lying countries such as the Netherlands. To ensure adequate safety against flooding, we assess and design dikes according to recently established risk-informed safety standards in terms of acceptable probabilities of flooding (see Jonkman, Voortman, Klerk, & van Vuren, 2018; Schweckendiek, Vrouwenvelder, Calle, Kanning, & Jongejan, 2013). One of the main failure mechanisms that can lead to dike breaching and subsequently flooding is slope instability.

The reliability of a dike slope can be estimated, for example, by means of a probabilistic slope stability analysis. Such analysis explicitly considers uncertainty in geologic, ground and geotechnical models quantitatively (e.g., Babu & Murthy, 2005; Cao, Wang, & Li, 2017; Ching, Phoon, & Hu, 2009; Christian, Ladd, & Baecher, 1994; Griffiths, Huang, & Fenton, 2009; Juang, Zhang, Shen, & Hu, 2019, Vanmarcke, 1980; Zhang, Zhang, & Tang, 2005). The dominant factors that determine the reliability estimates of slope stability are soil properties, which are uncertain due to spatial variability, measurement errors, transformation errors or sparse data (see Cao et al., 2017; Phoon & Kulhawy, 1999a, 1999b), and pore water pressures. In contrast to inherent variability, epistemic uncertainty can be reduced by including additional information using Bayesian analysis (e.g., Baecher & Christan, 2003; Straub & Papaioannou, 2014).

Past performance (e.g. the survival of a loading condition) is one example of additional information that can be used to improve reliability estimates. For instance, Zhang, Zhang, and Tang (2011) and Li et al. (2015) considered the survival of a phreatic level. Schweckendiek (2010) and Schweckendiek, Vrouwenvelder, and Calle (2014) considered historically survived flood water levels. These studies have shown that the reliability estimate can increase significantly when a critical load has been survived. However, observations of survived critical loading conditions such as extreme flood water levels are rare, and hence, not always available. Instead, we may consider another potentially critical and more widely available loading condition for dikes: the construction.

During the construction of embankments on soft soils in general, and dikes in particular, the stability typically reaches critical levels. The main cause is the resulting excess pore water pressure in the foundation as the embankment is raised. Baecher and Ladd (1997) showed that performance information of survived construction stages can be used to update the slope stability predictions in later construction stages. That

* Corresponding author at: Faculty of Civil Engineering and Geosciences, Delft University of Technology, Delft, The Netherlands.
E-mail address: M.G.vanderkrogt@tudelft.nl (M.G. van der Krogt).

https://doi.org/10.1016/j.enggeo.2020.105937
Received 17 July 2020; Received in revised form 29 October 2020; Accepted 29 November 2020
Available online 5 December 2020

case study, however, only considered the stability during the construction, not flood loading.

The objective of this paper is to examine how the survival of the construction stage can be used to improve the reliability estimates of dike slopes in flood conditions. A practical approach using Bayesian Updating is proposed to incorporate the observation of construction survival in the reliability analysis. The approach is exemplified for a range of typical dikes and for a case study of a full-scale test embankment. The presented case studies reveal insights into the conditions in which we can expect a significant increase in the reliability estimate. And thus, in which cases it is worthwhile to consider a reliability analysis with Bayesian updating.

The paper is structured as follows. First, we compare the factors of safety at the end of construction with the factors of safety in flood conditions for a range of hypothetical cases of typical dikes. This indicates for which cases the construction of a dike is a critical loading condition. Then, we propose a practical approach to incorporate construction survival in the probabilistic analysis of a dike in flood conditions using Bayesian updating. Next, the effect of including construction survival on the reliability estimate is investigated for the different cases, under various hypothetical survived conditions. Furthermore, we present a case study of a recently constructed dike, demonstrating the practical applicability of the proposed approach. The paper concludes with a discussion on how the approach can be applied in practice and which further developments are desirable.

2. Dike construction as critical loading condition

The construction of a dike is one of the loading conditions to which a slope and subsoil may be subjected, when regarding the safety with respect to slope stability (USACE, 2003). Raising an embankment leads to excess pore water pressures in soft soil foundation layers (see Fig. 1b), resulting in low effective stresses. Due to feasibility and economic reasons, critical levels of stability (low factors of safety) are often accepted during the construction of dikes; all the more because potential damage in terms of loss of life and injuries during construction is usually low, compared to the design conditions.

If dike construction is a critical loading condition, then survival of this loading condition provides additional information about the shear strength properties involved. 'Construction survival' is the observation that no slope instability has occurred under the loading conditions during the construction phase. The corresponding information is that the factor of safety must have been greater than 1.0 at the time of the observation. Field observations to substantiate observations of construction survival can be the absence of cracks or excessive deformations, or other monitoring indicating that a rotational shear failure was not initiated under de observed loading conditions (Tavenas, Mieussens, and Bourges (1979) describes some of those).

The question is, however, what construction survival tells about the reliability under the design loading conditions of a dike, namely flood loading. Although flood loading and the construction seem to be two different loading conditions, they are in fact quite similar. First of all because the main load effect in terms of increased pore water pressures is, in principle, comparable. Secondly, in both cases potential slip planes intersect the dike body and mostly the same subsoil layers.

There are, of course, differences. For example, the pore water pressures during flood loading are induced by seepage and mainly affect the dike body. The pore water pressures in the soft foundation soil are typically less affected, depending mainly on the flood duration. In contrast, the main increase in pore pressure during construction occurs in the soft soil foundation below the dike.

However, slightly lower effective stresses do not necessarily lead to significantly lower undrained strength of over-consolidated soil, as pointed out by Shewbridge and Schaefer (2013). The undrained shear strength is therefore quite similar in both loading conditions. Moreover, the information of construction survival can be related to an update of the underlying soil parameters, instead of the shear strength itself. For example when using Critical State Soil Mechanics (CSSM) and Stress History and Normalized Soil Engineering Properties (SHANSEP).

2.1. Deterministic sensitivity study characteristic dike profiles

In order to sort out in which situations the construction phase is indeed a critical loading condition compared to the design loading conditions, we compared the respective factors of safety for five hypothetical, typical dike cross sections (outlined in Fig. 2). These typical cases cover different combinations of subsoil (thick clay layer on sandy subsoil, thin clay layer on sandy subsoil, and only sand subsoil) and dike material (clay or sand with a clay cover). For the cases with a clay layer, we distinguish cases with normally consolidated (NC) versus over-consolidated (OC) soil. All cases involve a dike height of 4.0 m and a 1:4 slope (v:h). The five cases certainly do not cover all possible cases. The cases are typical for the Dutch situation, but also characteristic for other locations, especially in deltaic areas.

The soil shear strength is modeled according to the CSSM framework (Schofield & Wroth, 1968) because the critical state concept suits best to a situation of continuous shear deformation along an entire slip plane (with large strains and no peak strength). The shear strength of the sand foundation layer and the unsaturated part of the dike body are modeled with a critical state friction angle φ_{cs}. The undrained shear strength (s_u) of saturated clay is modeled with the SHANSEP formulation (Ladd & Foott, 1974):

$$s_u = \sigma'_v \cdot S \cdot OCR^m \quad (1)$$

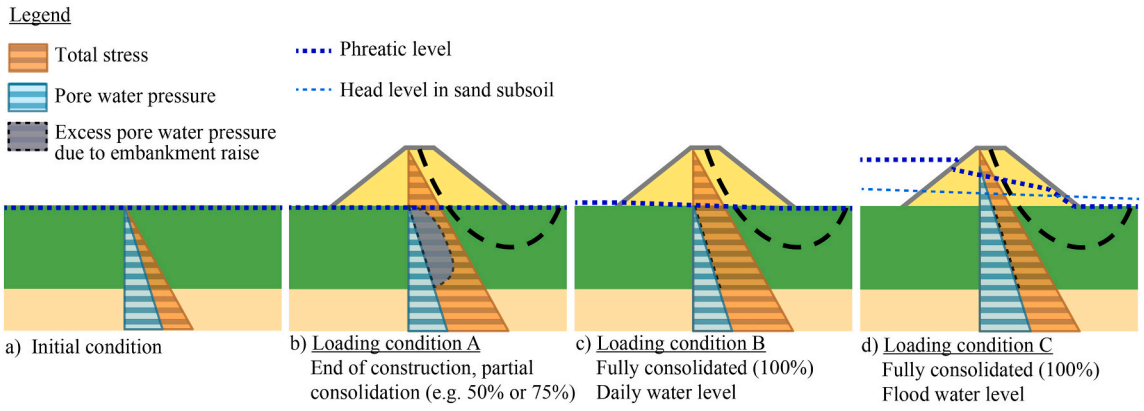

Fig. 1. Overview of different loading conditions of a sand dike (with clay cover) on a soft soil blanket layer and sand subsoil. The typical failure mechanism (slip plane) is indicated with the dashed line.

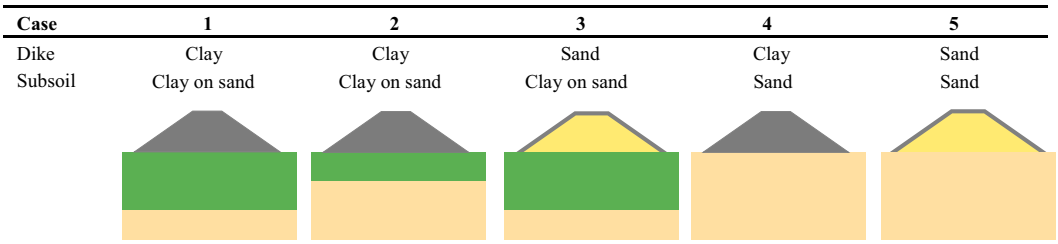

Fig. 2. Overview of characteristic dike profiles. Grey and green indicate clay soil (for the dike core and subsoil, respectively). Yellow and orange indicate sand soil (for the dike core and subsoil, respectively). (For interpretation of the references to colour in this figure legend, the reader is referred to the web version of this article.)

Here, S = undrained strength ratio for normally consolidated soil, m = strength increase exponent, and OCR = over-consolidation ratio, being the ratio of in situ vertical effective stress σ'_v and preconsolidation stress $\sigma'_p = \sigma'_v + POP$, where POP = pre-overburden pressure.

The probability distributions of the soil properties (see Table 1) have been chosen such that they represent realistic probability distributions, resembling what is typically encountered in the field. Spatial variability is implicitly modeled in the parameter distributions, by modeling spatial average soil properties. The mean and standard deviations are in line with values reported in various case studies (e.g., Berre & Bjerrum, 1975; Ochiai, 1980; Ladd, 1991, Baecher & Ladd, 1997, Watabe, Tsuchida, & Adachi, 2002, Stuedlein, Kramer, Arduino, & Holtz, 2012, De Koning et al., 2019).

The factor of safety F_s has been examined for three consecutive loading conditions: (A) end of construction, (B) full consolidation with daily water levels, and (C) full consolidation with flood water levels; see Fig. 1b-d.

Loading condition A is immediately after finishing the construction of the dike. As a result of the staged construction process. Excess pore pressures are still present in the clay foundation layers. In real-life situations we would use actual pore water pressure data to estimate the degree of consolidation (i.e. the dissipated excess pore water pressures in the foundation). For the hypothetical cases we assumed typical average degrees of consolidation of 50% and 75% to study the sensitivity to this parameter. Although the actual excess pore pressure varies with depth, we modeled a constant excess pore water pressure distribution over the soil layer. This represents the average degree of consolidation along potential slip planes. The phreatic level at the end of construction is assumed to be at surface level, and the dike body unsaturated. The construction is assumed to be with a new material with no significant unsaturated contribution to the shear strength (e.g. no suction forces) leading to the assumption that the unsaturated contribution in the construction phase is neglected.

Loading condition B is defined as the situation when the subsoil has been fully consolidated. In this situation all excess pore pressures have dissipated. The phreatic level is at surface level, identical to loading condition A. Loading condition C considers the dike with a fully consolidated subsoil in flood conditions, with steady-state seepage conditions (i.e. largely saturated dike body and increased head in the foundation layers, schematically indicated in Fig. 1d).

The slope stability has been calculated with the Limit Equilibrium method (LEM) Bishop (Bishop, 1955), using the D-Stability software (Deltares, 2018a). Advantages of the LEM method compared to more advanced models are its simplicity, robustness, and the favorable computation time. Although advanced methods might predict deformations of a slope better, they usually require more computation time and are less robust (e.g. Juang, Gong, Martin, & Chen, 2018). Moreover, the deformations are not of interest in this paper, since the main focus is on predicting the slope stability.

All factors of safety F_s presented throughout this paper are calculated with the expected values of all random variables. Excess pore water pressures during construction are taken into account in the calculation of the effective stress per slice. Seepage is considered through a gradient over the slices in the LEM model.

Fig. 3 confirms that the slope stability increases with increasing consolidation (from loading condition A to B), for dikes on clay (cases 1–3). For a sand foundation layer, we consider no significant excess pore pressures. Hence, there is no difference in F_s between loading conditions A and B in cases 4 and 5.

The most important observation in reliability updating context is that the stability at the end of construction is in many cases much lower than during flood conditions. For dikes on a clay foundation (cases 1–3), the F_s in loading condition A is in almost all cases lower than the F_s in loading condition C. The reason is that for dikes on a clay foundation the subsoil is not fully consolidated at the end of the construction, unlike for sand. Hence, cases 4 and 5 do not show a lower stability at the end of

Table 1
Probability distributions of soil properties used in the case studies. The probability distributions resemble values which are typically encountered in the field, in line with values reported in various case studies: e.g., Berre & Bjerrum, 1975; Ochiai, 1980; Ladd, 1991, Baecher & Ladd, 1997, Watabe et al., 2002, Stuedlein et al., 2012, De Koning et al., 2019.

Soil	Volumetric weight γ_{sat}/ γ_{unsat} [kN/m3]	Normally consolidated undrained shear strength ratio S [-]	Strength increase exponent m [-]	Pre-overburden pressure[a] POP [kPa]	Critical state friction angle φ_{cs} [degrees]
Dike Clay[b]	17/17	Lognormal μ 0.30, σ 0.03	Deterministic 0.80		Lognormal μ 32, σ 3.2
Dike Sand	17/19				Lognormal μ 32, σ 3.2
Clay NC	14/14	Lognormal μ 0.30, σ 0.03	Deterministic 0.80	Lognormal μ 10, σ 2.0	
Clay OC	14/14	Lognormal μ 0.30, σ 0.03	Deterministic 0.80	Lognormal μ 30, σ 6.0	
Sand	18/20				Lognormal μ 35, σ 1.75

[a] The pre-overburden pressure (POP) refers to a the initial situation, before construction of the dike. A normally consolidated (NC, POP = 10 kPa, $OCR \approx$ 1–3) and over consolidated (OC, POP = 30 kPa, $OCR \approx$ 3–5) situation is distinguished.

[b] Saturated Dike Clay is modeled using SHANSEP parameters S, m and POP (or OCR), unsaturated Dike Clay is modeled using a critical state friction angle φ_{cs}.

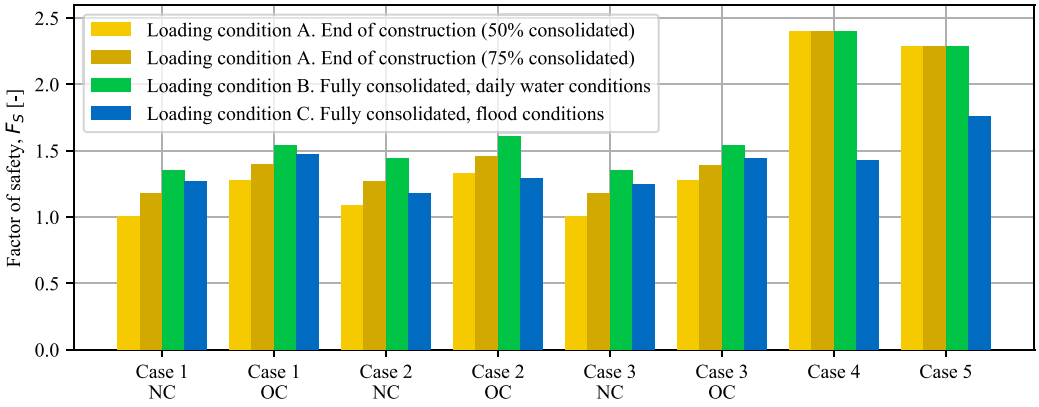

Fig. 3. Factor of safety for slope stability considering different loading conditions for various typical dike profiles with normally consolidated (NC) and over-consolidated subsoil (OC). For dikes on clay subsoil (cases 1–3), the stability at the end of construction is much lower than during flood conditions.

construction than during flood conditions.

For dikes on a thin soft soil foundation (case 2), the difference in F_s between the end of construction and flooding conditions is less than in other cases (case 1 and 3). The reason is that water pressures in the foundation sand layer during floods have a greater influence on the stability in case 2.

For dikes on soft soil foundation layers, we may thus expect that incorporating construction survival will yield an increased reliability estimate. Vice versa, for the dikes on sand subsoil, we do not expect a significant effect on the reliability, and therefore cases 4 and 5 are not considered in the further analysis.

3. Reliability updating with construction survival

To incorporate construction survival in the probabilistic analysis of a dike in flood conditions, a practical approach is proposed. The approach is based on probabilistic slope stability calculations and Bayesian updating. Since the factor of safety F_s indicates the ratio of resistance over load, instability occurs in a perfect model if $F_s < 1.0$. Contrary, a slope is stable if $F_s \geq 1.0$, presuming that slopes with $F_S = 1.0$ are also just stable. To account for model error, F_s is multiplied with a model uncertainty factor d. Accordingly, the limit state function g is generally defined as

$$g(\mathbf{x}) = F_s \cdot d - 1 \tag{2}$$

Herein, $\mathbf{x}$ is a realization of $\mathbf{X}$, with $\mathbf{X}$ the vector of all (random) variables. Note that we do not explicitly distinguish between the input parameters of the model to calculate F_s (i.e. soil parameters, pore pressures, etc.) and the model uncertainty d, in this notation. The probability of failure is generally defined as:

$$P_f = \int_{g(\mathbf{x})<0} f_{\mathbf{X}}(\mathbf{x}) d\mathbf{x} \tag{3}$$

where $f_{\mathbf{X}}(\mathbf{x})$ the probability density of $\mathbf{X}$ for a realization $\mathbf{x}$, and $g(\mathbf{x}) < 0$ denotes the failure domain.

More specifically for the envisaged application, we define $\mathbf{X}_A$ for a dike in the assessed flood conditions, and $\mathbf{X}_S$ for the survived construction. Note that $\mathbf{X}_A$ and $\mathbf{X}_S$ contain the same variables, but they represent the states of the variables at different moments in time, namely the assessed flood conditions and survived construction. Many of them are time-invariant soil properties which are modeled as fully correlated between the assessed flood conditions and the survived construction. Other variables (such as pore pressures) are independent/uncorrelated between the assessed and survived situation.

Let F be the event of slope failure in the assessed loading condition B or C (i.e., daily or flood water level, respectively), where $g(\mathbf{x}_A) < 0$ the domain of failure in the assessed loading condition, and $\mathbf{x}_A$ a realization of $\mathbf{X}_A$. The probability of failure (further referred to as prior probability) is given by

$$P(\mathrm{F}) = \int_{g(\mathbf{x}_A)<0} f_{\mathbf{X}_A}(\mathbf{x}_A) d\mathbf{x}_A \tag{4}$$

where $f_{\mathbf{X}_A}$ the probability density of $\mathbf{X}_A$. Similarly, let ε be the event of construction survival, thus where $g(\mathbf{x}_S) \geq 0$ the domain of survival with the survived loading conditions, and $\mathbf{x}_S$ a realization of $\mathbf{X}_S$. Hence, the probability of survival is given by

$$P(\varepsilon) = \int_{g(\mathbf{x}_S)\geq 0} f_{\mathbf{X}_S}(\mathbf{x}_S) d\mathbf{x}_S \tag{5}$$

To incorporate construction survival in the probabilistic analysis of a dike in flood conditions, Bayesian updating is used. Zhang et al. (2011) distinguishes two methods to incorporate performance information: the indirect method and the direct method. In the indirect method, the parameter distribution $f_{\mathbf{X}_A}$ is first updated to $f_{\mathbf{X}_A|\varepsilon}$, using the likelihood of survival $L(\mathbf{x}_A) = P(\varepsilon | \mathbf{X}_A = \mathbf{x}_A)$, see Eq. (6). Thereafter the failure probability is recalculated using this updated distribution, see Eq. (7).

$$f_{\mathbf{X}_A|\varepsilon}(\mathbf{x}_A) = \frac{L(\mathbf{x}_A) f_{\mathbf{x}_A}(\mathbf{x}_A)}{\int_{\mathbf{X}_A} L(\mathbf{x}_A) f_{\mathbf{x}_A}(\mathbf{x}_A) d\mathbf{x}_A} \tag{6}$$

$$P(\mathrm{F}|\varepsilon) = \int_{g(\mathbf{x}_A)<0} f_{\mathbf{X}_A|\varepsilon}(\mathbf{x}_A) d\mathbf{x}_A \tag{7}$$

In a survived situation, the exact value of F_s cannot be identified, but we do know that factor of safety was larger than 1.0 under those loading conditions. The survival observation therefore provides inequality information, for which the likelihood function takes the value 1 if a realization is in accordance with the observation. When a realization it not in accordance with the observation, the likelihood takes the value 0, as formulated in Straub and Papaioannou (2014).

The direct method, on the other hand, is a direct application of the Bayes' theorem and is defined in terms of conditional probability, see Eq. (8).

$$P(\mathrm{F}|\varepsilon) = \frac{P(\mathrm{F} \cap \varepsilon)}{P(\varepsilon)} = \frac{P(g(\mathbf{X}_A) < 0 \cap g(\mathbf{X}_S) \geq 0)}{P(g(\mathbf{X}_S) \geq 0)} \tag{8}$$

Although the two methods have a different formulation, they have the same theoretical basis (Bayes Theorem). Both methods have their opportunities, depending on the implementation and application. The indirect method is particularly favorable when information relates to

best estimates, and parameter distributions can be easily reconstructed, for example, through updated values of the distribution parameters (e.g. Jiang, Huang, Qi, & Zhou, 2020). Survival information, however, usually relates to unlikely combinations of parameters and the tail of the joint parameter distribution (discussed later in this paper, Fig. 6). In such situations it may be more difficult to accurately reconstruct the posterior probability distributions. In this paper the main attention is to the reliability update, and not the updated probability distributions. Therefore, we use the direct method.

3.1. Implementation with Crude Monte Carlo

The posterior probability can be estimated using Crude Monte Carlo by counting the number of realizations in the failure domain, where we only take into account the realizations for which the construction has been survived. Thus if $g(\mathbf{x}_{A,i}) < 0 \cap g(\mathbf{x}_{S,i}) \geq 0$ for realizations $\mathbf{x}_{A,i} \in \mathbf{X}_A$ and $\mathbf{x}_{S,i} \in \mathbf{X}_S$. Using the indicator function $1[\cdot]$, we estimate the posterior probability as follows:

$$P(\mathrm{F}|\varepsilon) \approx \frac{\frac{1}{n}\sum_i^n 1\left[g\left(\mathbf{x}_{A,i}\right) < 0 \cap g\left(\mathbf{x}_{S,i}\right) \geq 0\right]}{\frac{1}{n}\sum_i^n 1\left[g\left(\mathbf{x}_{S,i}\right) \geq 0\right]} \tag{9}$$

Although a single slope stability calculation to evaluate the limit state function g does not require much computation time, evaluating a large sample becomes computationally expensive – especially for low probabilities. Therefore, we propose an approximation to evaluate the outcome of $g(\mathbf{x}_{A,i}) < 0$ and $g(\mathbf{x}_{S,i}) \geq 0$. To that end, we first replace $g(\mathbf{x}_{A,i}) < 0$ and $g(\mathbf{x}_{S,i}) \geq 0$ by indicator functions $\chi_{F,i}$ and $\chi_{\varepsilon,i}$, respectively. Since indicator functions only take values 1 or 0, the AND-gate ($\cap$) can be replaced by the logical operation of a parallel system: a multiplication. The 1/n terms drop from the equation, and the posterior probability of failure is written as follows:

$$P(\mathrm{F}|\varepsilon) \approx \frac{\sum_i^n \chi_{F,i} \cdot \chi_{\varepsilon,i}}{\sum_i^n \chi_{\varepsilon,i}} \tag{10}$$

We approximate the outcome of the indicators $\chi_{F,i}$ and $\chi_{\varepsilon,i}$ based on the prior probabilities for failure and survival. This is done by comparing realizations of the standard uniform variables u and v with the previously calculated probabilities $P(\mathrm{F})$ and $P(\varepsilon)$:

$$\chi_{F,i} = 1[u_i < P(\mathrm{F})] \tag{11}$$

and

$$\chi_{\varepsilon,i} = 1[v_i > P(\varepsilon)] \tag{12}$$

This principle is similar to generating random realizations using the inverse cumulative distribution function. The main advantage of this method is that we only have to carry out stability analyses to estimate $P(\mathrm{F})$ and $P(\varepsilon)$, and not $P(\mathrm{F} \cap \varepsilon)$. The $P(\mathrm{F})$ and $P(\varepsilon)$ may be evaluated for example by methods that require fewer model evaluations, such as FORM (First Order Reliability Method, Hasofer & Lind, 1974). The calculation of $P(\mathrm{F} \cap \varepsilon)$ on the other hand, would require more advanced reliability methods with more model evaluations.

Since $\mathbf{X}_A$ and $\mathbf{X}_S$ are correlated due to the subset of time-invariant variables they have in common, the realizations of the limit state functions $g(\mathbf{x}_A)$ and $g(\mathbf{x}_S)$ are correlated. This is taken into account by simulating equally correlated values of u_i and v_i. In fact, this is the application of the Equivalent Planes Method (Roscoe, Diermanse, & Vrouwenvelder, 2015). The correlation $\rho_{u,v}$ can be estimated from the influence coefficients α_k of the FORM calculation of $P(\mathrm{F})$ and $P(\varepsilon)$) for all parameters k, considering the autocorrelation of those parameters ρ_k, see Eq. (13). The autocorrelation depends, among others, on which parameters are variable in time, as discussed in the next section. The effectiveness of the practical approach using indicators and the approximation of the correlation is discussed in Section 4.4.

$$\rho_{u,v} \approx \sum_k \alpha_k^A \cdot \alpha_k^S \cdot \rho_k \tag{13}$$

3.2. Reducible uncertainty

Although the survived and assessed situations are largely comparable, mainly because the soil properties are time-invariant, there are differences between the two situations. Therefore, we cannot guarantee with certainty that any flood situation will be survived when the construction was survived, even though the calculated F_s would suggest a less critical loading under flood conditions.

The extent to which uncertainty can be reduced (and reliability can increase) depends on whether the uncertainty in the parameters is epistemic, and hence, reducible, and whether the parameters are time-invariant, or not. To this end, we distinguish between random variables addressing predominantly epistemic uncertainty (due to a lack of knowledge) and random variables modeling aleatory uncertainty (i.e. actual randomness in time).

The uncertainty in soil properties is arguably of predominantly epistemic nature because most uncertainty relates to a lack of knowledge about the exact value, for example, due to limited soil investigation. Soil properties are also assumed to be time-invariant, i.e. identical in the survived and assessed situation. This is taken into account by assuming full autocorrelation ($\rho_k = 1$) for each time-invariant parameter k in Eq. (13).

For other stochastic parameters the values can differ between loading conditions, for example the phreatic level, the shear strength of unsaturated versus saturated clay, and the model uncertainty factor. Hence, information on the survived conditions does not give information about those parameters in flood conditions. Therefore, no autocorrelation ($\rho_k = 0$) has been assumed for time-variant stochastic parameters.

4. Case study characteristic dike profiles

This section examines the impact of incorporating construction survival in the reliability estimate at daily and flood conditions (loading condition B and C). To that end, the reliability (conditionally to daily and flood water levels) was estimated with and without construction survival for the characteristic dike profiles. First the case input is described, then the reliability results are presented. Next, a sensitivity study regarding different survived conditions is presented to address the influence of OC and NC soil on the reliability update. Then the effectiveness of the proposed approach is discussed. The last section summarizes the influences of the specific dike profiles on the reliability updating.

4.1. Case description

The prior probability of slope instability (conditional on the considered loading condition) was estimated using FORM because it can reach accurate results with limited computational time, (e.g., De Koker, Day, & Zwiers, 2018; Huber, van der Krogt, & Kanning, 2016; Kanning et al., 2017). The prior probability distributions are shown in Table 1. In this study we used a lognormal distribution with $\mu = 1.0$ and $\sigma = 0.05$ for the model uncertainty factor d. We assumed an unbiased model, since most of the model error contributions (3D-effects, appropriateness of strength data, strain-compatibility, etc.) are likely to cancel each other out (Ladd & Degroot, 2003). The standard deviation represents a central value in the range from 0.02 to 0.10 found in literature (e.g., Azzouz, Baligh, & Ladd, 1983; Christian et al., 1994; Ladd & Degroot, 2003).

The soil properties S, m, POP, and φ_{cs} are assumed to be time-invariant parameters, for which full autocorrelation is assumed ($\rho_k = 1$). The model uncertainty factor and the phreatic level (and pore water pressures) are assumed to be time-invariant, so these were

independently modeled in the assessed and survived situation ($\rho_k = 0$). Although the drained and undrained strength of the dike material is correlated to some extent, we assumed that the drained (φ_{cs}) and undrained strength parameters (S, m, POP) of the same soil are uncorrelated ($\rho_k = 0$), in order to not overestimate the effect of updating in this regard.

4.2. Reliability results

Fig. 4 shows the reliability index for the considered cases, with and without incorporating construction survival (with 50% consolidation at the end of the construction). Incorporating construction survival leads to an increase in reliability in all cases, but the reliability updating effect differs from case to case. For the daily water level, the posterior probability of failure is a factor 10 to 1000 lower than the prior probability of failure. For the flood water level, the reduction in failure probability is a factor 2–70.

The impact on the reliability at flood conditions is lower than conditional on the daily water level. This is mainly a result of a lower correlation between the design situation and the survived situation, because the load effects (specifically the pore water pressures) are different between the situations. For example, in case of thin blanket layers, such as in case 2, pore water pressures in the sand foundation have a large effect on the shear strength, which makes flood loading conditions quite different from the construction conditions. Consequently, the survival of the construction provides little extra information about the stability in flood conditions, and therefore, the impact on the reliability is low.

The results, however, are presented conditional to the water level, whereas the total probability of failure is the probability-weighted sum of the conditional failure probabilities for all water levels in the relevant range; two of which are considered by loading condition B and C. To provide a rough estimate of the total annual failure probability for the characteristic dike cases, we combined the conditional failure probabilities $P(F) \mid h$ with the probability density of the water level $f(h)$, using the approach in Schweckendiek et al. (2017). We used a Gumbel-distributed probability distribution of the water level based on the assumption that the flood level of loading condition C corresponds to an exceedance probability of 1/100 per year. Due to the larger effect of the survival information on lower water levels (which have the highest probability density), the annual reliability increases significantly, see Table 2. This demonstrates that the increase in the total reliability can be still significant, even though the effect of reliability updating on the conditional reliability for flood conditions is limited.

4.3. Influence of OC and NC soil on the reliability update

It is striking that the reliability update in all cases with NC soil is much higher than in the cases with OC soil. This is explained by the relatively high probability of failure for the dikes on weak NC soil considered in this example, compared to dikes on OC soil, see Table 2.

Table 2
Failure probability at the end of construction, and prior and posterior annual reliability estimates of slope stability for the characteristic dike profiles considered.

Case Study	Failure probability Loading condition A: End of construction	Reliability index β (probability-weighted sum of the conditional failure probabilities for all water levels)		Ratio prior/ posterior failure probability
		A priori (without construction survival)	A posteriori (with construction survival)	
Case 1, NC	0.49	2.97	4.26	146
Case 1, OC	0.02	4.04	4.52	9
Case 2, NC	0.21	3.37	3.96	10
Case 2, OC	0.01	4.23	4.40	2
Case 3, NC	0.49	2.93	4.49	476
Case 3, OC	0.02	4.01	4.57	12

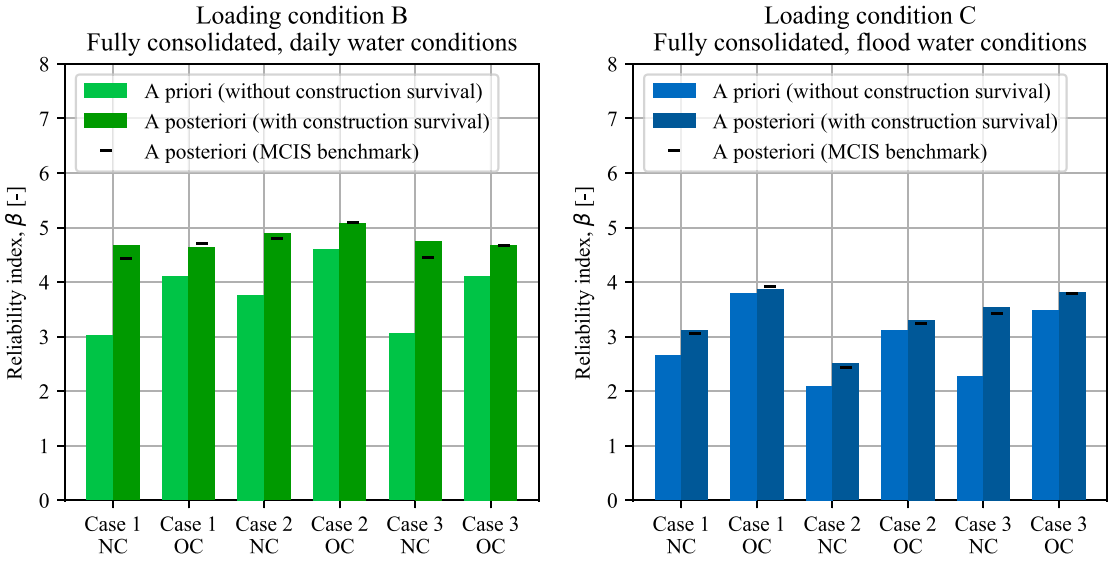

Fig. 4. Prior and posterior reliability index of slope stability (with and without construction survival with 50% consolidation at the end of the construction, respectively). Results are shown conditional to daily (left) and flood water levels (right). The bars show the results obtained with the proposed simplified method in this paper; the horizontal black lines show benchmark results obtained with Monte Carlo Importance Sampling (MCIS).

This is in accordance with the F_s close to 1.0 during construction (Fig. 3) and confirms earlier findings that the reliability update depends among others on the criticality of the survived situation.

However, remarkably, it turns out that the update generally is higher in the cases with OC soil, at least when looking at roughly equally critical survived situations. This follows from a sensitivity study regarding the degree of consolidation at the end of construction (i.e. the dissipated excess pore water pressures in the foundation). From Fig. 5, it can be read at what degree of consolidation the probability of failure is more or less equal, and thus at which conditions the situations are equally critical. A failure probability of 0.01–0.05 is found at a degree of consolidation of 80% for the NC cases, and 50% for the OC cases in Fig. 5a. When regarding these survived conditions specifically, the posterior failure probabilities for dikes on NC soil are approximately a factor 4 lower than the prior failure probabilities, compared to roughly a factor 10 for dikes on OC soil, see Fig. 5b and c. The main reason for the larger update is that the total uncertainty is larger for dikes on OC soil, which is discussed in more detail in the next section.

The analysis further shows that significant reliability updates are possible, even when the probability of failure during construction is lower than 0.05; to our judgement a reasonable and generally accepted safety level during construction.

4.4. Validation of the proposed approach

To demonstrate the accuracy of the proposed approach based on the indicator function (using Eq. (10)), the results were benchmarked with Monte Carlo Importance Sampling (MCIS) (similar to Eq. (7), but with IS weighting factors). The results of the proposed method are in reasonable accordance with the MCIS results, depicted by black horizontal lines in Fig. 4.

From the MCIS it also follows that the correlation between realizations of the limit state functions $g(\mathbf{x}_A)$ and $g(\mathbf{x}_S)$ is very similar to the estimate based on Eq.(11). For example for case 1 NC, the Pearson correlation coefficient between loading condition B and A based on MCIS is 0.72, The estimate using Eq. (11) is 0.73. For loading condition C and A, the correlation coefficient is 0.56 based on MCIS, and 0.58 based on Eq. (11). Note that the correlation coefficient in the considered cases mainly depends on the choice about the autocorrelation of parameters (ρ_k). The contribution of different importance of parameters in both calculation is only minor. Similar results are found for the other cases. Therefore, the proposed approach is a convenient, practical alternative for estimating low posterior conditional probabilities of failure.

The Monte Carlo analysis further provides insights in how the information contained in the survival of construction leads to uncertainty reduction. Fig. 6 depicts the samples in the Monte Carlo analysis which are not consistent with the observation (i.e. where $g(\mathbf{x}_{S,i}) < 0$). The figure shows that survival information relates to unlikely combinations of parameters and the tail of the joint parameter distribution, for which a reconstruction of the posterior probability distributions generally is not too easy.

The figure shows that the largest contribution to the increase in reliability is due to the exclusion of unlikely combinations of *S* and *POP* of the clay layer for the OC cases. This is logical because the uncertainty in the pre-consolidation is large for OC soils. For the NC cases on the other hand, pre-consolidation obviously does not play a role as the pre-consolidation is almost directly exceeded by the embankment raise. Therefore, the shear strength is only determined by the relatively less

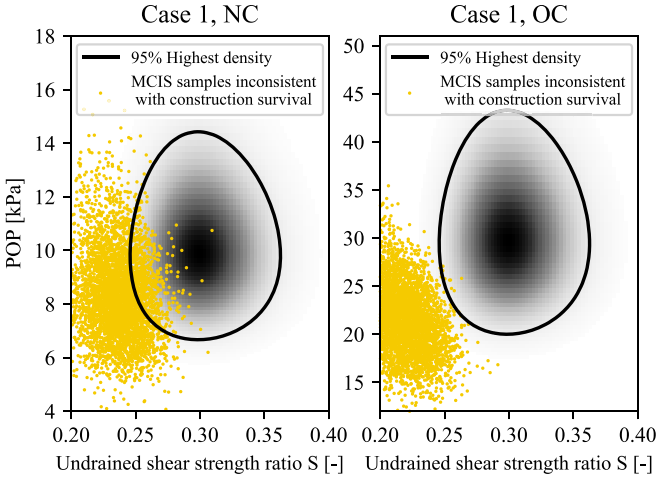

Fig. 6. Joint probability density (grey shading) for undrained shear strength ratio (*S*) and POP values. Yellow dots show the realizations that are not consistent with the survived construction (i.e. for which$g(\mathbf{x}_{S,i}) < 0$). For the NC case, the uncertainty reduction is mainly in undrained shear strength ratio (*S*). For the OC case, the uncertainty reduction is mainly in combinations of *S* and POP of the clay layer. (For interpretation of the references to colour in this figure legend, the reader is referred to the web version of this article.)

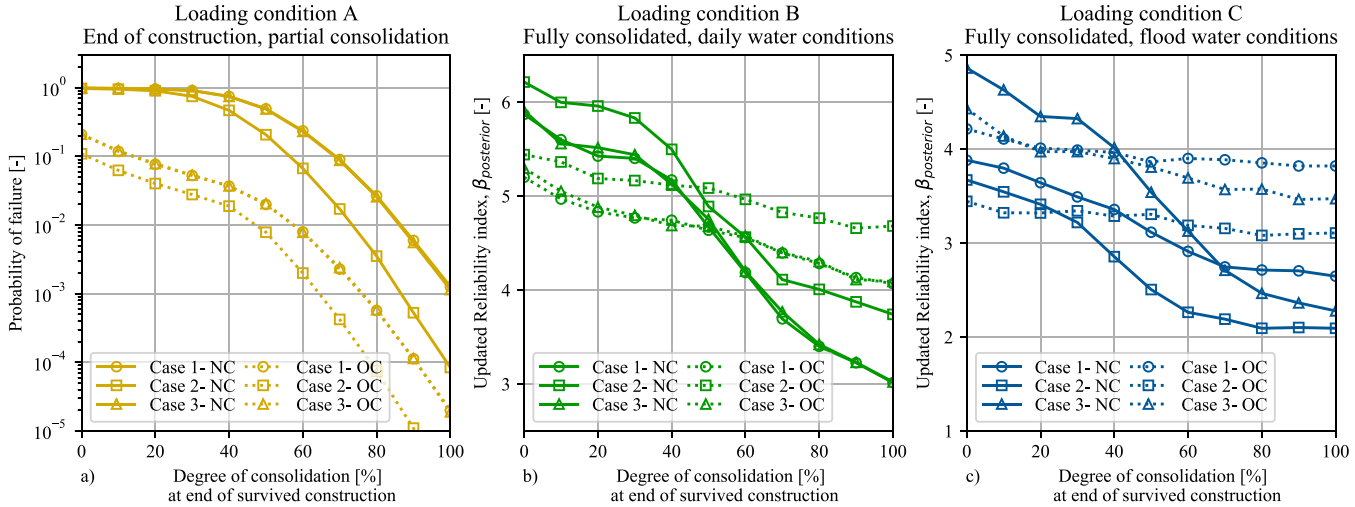

Fig. 5. Influence of the survived degree of consolidation at the end of construction on the updated reliability for slope stability of different cases. The left graph (a) shows the probability of failure after construction, the middle graph (b) the updated reliability index conditional to daily water level, the right graph (c) conditional to flood water levels.

uncertain undrained shear strength ratio (S). Hence, in the NC cases, the S of the clay layer is updated mostly.

4.5. Summary

Based on the presented results, the following conclusions are drawn regarding the influence of the considered characteristic dike cases on the reliability update:

- For dikes on a sand foundation (case 4 and 5), the construction is not a critical load because excess pore water pressures dissipate almost instantaneously during construction. Hence, no reliability update is expected from incorporating construction survival.
- In case 2, the presence of a relatively thin clay blanket layer leads to considerably different pore water pressures in the subsoil at flood loading conditions than during the survived conditions. This limited similarity between loading conditions results in a lower reliability update effect.
- For dikes on OC soil, the effect of incorporating construction survival turned out to be generally larger than for dikes on NC soil. The main reason is the larger uncertainty in properties of OC soil, leading to more uncertainty reduction. In the cases with dikes on NC soil, the uncertainty was smaller, thus less uncertainty could be reduced.
- No firm conclusions can be drawn about the influence of different dike materials. Although the material properties and pore pressures differ slightly between the clay dike (case 1) and the sand dike (case 3), the main uncertainty is in the shear strength of the soft soil blanket. And hence, the reliability update in both cases is mainly due to uncertainty reduction in the soft soil parameters, not the dike material parameters.

5. Case study of the Eemdijk test dike

This section demonstrates the application of the proposed approach to a real dike in Eemdijk, The Netherlands (see Fig. 7). The case study concerns a full-scale test of two dikes, one conventional dike and one dike reinforced with a sheet pile wall. Both dikes were loaded until failure, with the main objective of validating models for slope failure of dikes with and without sheet piles (Lengkeek, Post, Breedeveld, & Naves, 2019). In contrast to the previous sections, this case study uses the actual data from site investigation and pore water pressure monitoring.

Fig. 7. Aerial photo of the Eemdijk ring-shaped test dike, with slope instability of the conventional (ground) dike (left). The test dike with sheet pile, is located on the right side. Image courtesy of Eric Feijten/NOS (Feijten, 2018).

5.1. Case description

The subsoil of the Eemdijk test dike consists of a 1.75 m thick clay layer, and a 2.5 m thick peat layer on top of a 6 m Pleistocene sand layer (see Fig. 8). The original surface level is at −0.1 m + N.A.P. (the local vertical datum: Amsterdam Ordnance Datum). The soil properties were obtained from laboratory tests (Deltares, 2018b), prior to the construction of the test dike. The undrained shear strength at specific locations was indirectly measured by cone penetration tests (CPTs), using a site-specific transformation model calibrated with laboratory tests (Van der Krogt & Schweckendiek, 2019). The stochastic soil properties are shown in Table 3. The dike, built of clean sand, 5.3 m high and slope 1:2 (v:h), was constructed in multiple stages (see Fig. 8) with no excessive deformations or cracks being observed. During construction, pore water pressures were continuously measured in the clay and peat layers at multiple locations.

5.2. Reliability results

Following the proposed approach, we calculated the prior reliability (without construction survival) and posterior reliability (with construction survival) of the test dike. The design conditions comprise different flood water levels and fully consolidated subsoil, as if the dike had been built as flood defense. The survived conditions are based on the actual measurement data acquired during construction (see Deltares, 2018c; Lengkeek et al., 2019). This involves data such as the geometry, phreatic level and the excess pore water pressures over the soil layers. The degree of consolidation below the dike was approximately 60%. The Uplift-Van model (Van, 2001) was used to calculate the factor of safety because of the possibility of uplift at the toe.

Fig. 9 shows that the failure probability for the daily phreatic level reduces significantly (factor 13 lower) by considering the survival of the last two construction stages. The effect of incorporating the survival information on the failure probability is negligible for design conditions with fully consolidated subsoil and a very high phreatic level. This is in line with the deterministic analyses reported in Table 4 because the factor of safety in the design conditions is lower than the stability during construction.

These results, however, are conditional failure probabilities. Therefore, we combine the conditional reliability indices in Fig. 9 with a probability density function of the phreatic level (the phreatic level virtually being the response to flood loading). A Gumbel distribution was used with annual exceedance probabilities of 1/2 and 1/100 for phreatic levels of 1.0 m + N.A.P. and 2.0 m + N.A.P., respectively. The combination results in a total prior annual reliability index of 1.59, and a total posterior annual reliability index of 2.51. This is a reduction in failure probability of almost one order of magnitude.

Similar to the cases of characteristic dikes, the total dike reliability estimate improves significantly, despite an insignificant reduction of the conditional failure probability at high water levels (i.e. design conditions). Again, the overall effect is due to the reduced conditional probability of failure for lower water levels, which are more similar and less critical than the observed loading conditions.

The effect of uncertainty in the measured excess pore water pressures at the survived loading conditions was investigated through a sensitivity analysis. From the data, a variation of the excess pore water pressure across the site was estimated 3 kPa. The influence on the posterior reliability of a 3 kPa higher or lower pore water pressure appears to be very limited, see the error bars in Fig. 9. In addition, the results obtained with Crude Monte Carlo simulation (using Eq. (7)) are in good accordance with the proposed approximation method.

5.3. Improved prediction for failure test

Instead of the dike being an actual flood defense (on fully consolidated soil as considered above), the failure test was executed directly

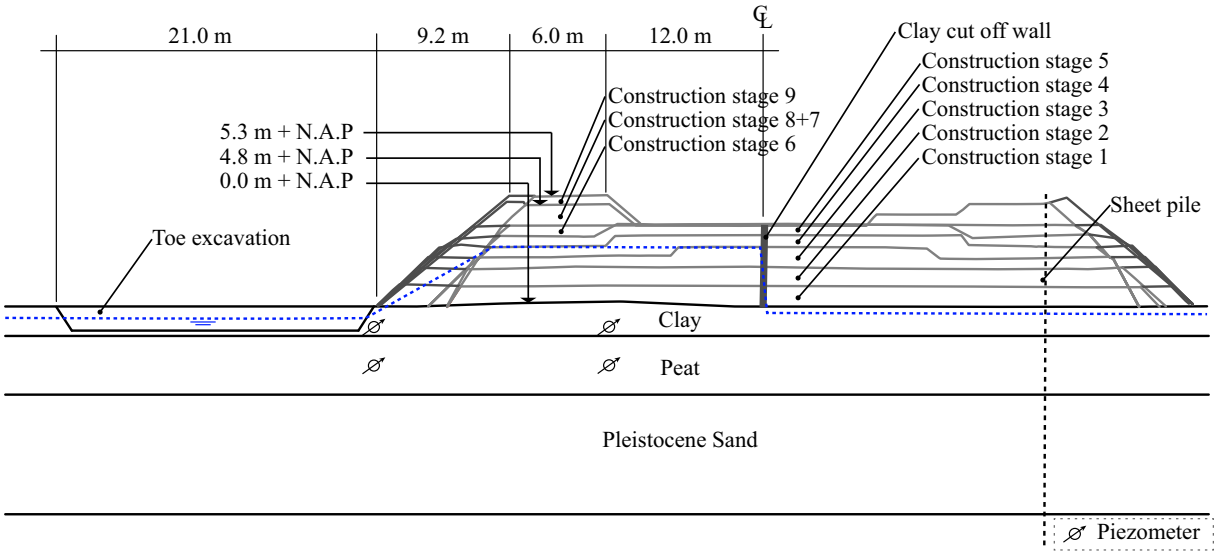

Fig. 8. Schematic overview of cross-section A-A' (see Fig. 5) of the Eemdijk test dike. The blue dotted line indicates the phreatic level during the failure test. Heights relative to Amsterdam Ordnance Datum (N.A.P.). (For interpretation of the references to colour in this figure legend, the reader is referred to the web version of this article.)

Table 3
Soil properties of the Eemdijk test site (Deltares, 2018b).

Soil	Property	Symbol	Distribution	Mean	Deviation	Type
Dike Sand	Friction angle	φ_{cs}	Log normal	35.0	1.5	S.D.
Clay	NC shear stress ratio	S	Log normal	0.38	0.05	S.D.
Clay	Strength increase exponent	m	Log normal	0.91	0.02	S.D.
Clay below crest[a]	Undrained shear stress (CPT)	s_u	Log normal	13.2	0.14[b]	V.C.
Clay below toe[a]	Undrained shear stress (CPT)	s_u	Log normal	6.2	0.14[b]	V.C.
Peat	NC shear stress ratio	S	Log normal	0.50	0.04	S.D.
Peat	Strength increase exponent	m	Log normal	0.87	0.03	S.D.
Peat below crest[a]	Undrained shear stress (CPT)	s_u	Log normal	24.6	0.19[b]	V.C.
Peat below toe[a]	Undrained shear stress (CPT)	s_u	Log normal	12.0	0.19[b]	V.C.
Sand Aquifer	Friction angle	φ_{cs}	Log normal	35.0	1.5	S.D.
Stability model	Model uncertainty (Deltares, 2015)	d	Log normal	0.995	0.033	S.D.

[a] The mean undrained shear strength under the dike crest differs from the toe as the area below the crest had been preloaded by an old, meanwhile removed dike.
[b] The uncertainty in the indirectly measured undrained shear stress (using CPT) before construction at a specific location is largely epistemic, since it includes a large transformation error (Van der Krogt & Schweckendiek, 2019; Van der Krogt, Schweckendiek, & Kok, 2018).

after the last construction stage, without full consolidation. The slope failure of the test dike was induced by increasing the phreatic level in the dike body, and additionally by excavating a trench adjacent to the dike toe (see Fig. 8). Consequently, the stability in terms of F_s during the failure test was lower than during construction (see Table 4). Nevertheless, the dike was critically loaded during construction (F_s was close to 1), thus considering construction survival should also improve the predicted performance during the failure test.

The reliability update for the failure test is depicted by the fragility curves in Fig. 10. Although the effect of considering construction survival is limited for the overall reliability (reduction by factor 2), the graph clearly shows the reduction of uncertainty by incorporating the construction survival. For example, it can be derived that the phreatic level at which $P(F) = 0.5$ (i.e. approximating the most likely loading condition triggering failure) increased from 1.0 m + N.A.P. (a priori) to 1.7 m + N.A.P. after updating. In the test, the slope eventually failed at a phreatic level of 2.9 m + N.A.P. Hence, we may conclude that the prediction of failure could be improved by using the information from the construction phase, even though we remain with an under-estimation of the slope resistance after updating.

6. Conclusion

This paper demonstrated that reliability estimates for dikes can be improved by considering the information contained in the survival of the often critical construction phase. Depending on the subsoil and loading conditions this can lead to a significantly higher posterior reliability, especially for dikes on undrained subsoil. The main reason is that the construction of dikes on soft soils is a critical loading condition, and the stability directly after construction is often lower than during the design flood conditions.

For several characteristic dike profiles, the (conditional) probability of failure reduced by a factor of 10 to 1000 for relatively low water levels. For high water levels representing design flood conditions, the impact was less significant with a reduction by a factor of 2 to 10. Primarily as a result of lower correlation or similarity between the survived and the assessed conditions. Nevertheless, the total dike reliability estimate (e.g., annual) can improve significantly because it considers the entire range of potential flood levels. Herein, extreme flood stages have a low probability of occurrence, and hence, a lower weight in the total reliability estimate.

The results obtained from the proposed approximation approach based on FORM calculations agree well with results obtained from Monte Carlo simulations, for conditional probabilities for the cases

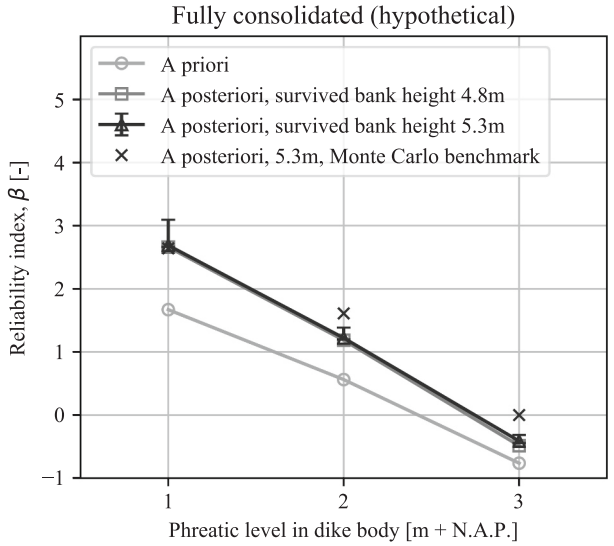

Fig. 9. Prior and posterior reliability index conditional to the phreatic level of a hypothetical design situation with a fully consolidated subsoil. Error bars show the influence of uncertainty in the measured pore water pressures (one standard deviation lower or higher) on the calculated posterior reliability.

Table 4
Factor of safety (F_s) in different loading stages and different phreatic levels relative to Amsterdam Ordnance Datum (N.A.P.). Mean values of the soil parameters are used.

	Phreatic level (relative to N.A.P. datum)			
Loading stages	0.25 m	1.0 m	2.0 m	3.0 m
Construction, 4.8 m bank height	1.03	N/A	N/A	N/A
Construction, 5.3 m bank height	1.02	N/A	N/A	N/A
Failure test	1.02	1.00	0.95	0.87
Failure test + toe excavation	0.92	0.90	0.85	0.76
Fully consolidated state (hypothetical)	1.17	1.13	1.05	0.94

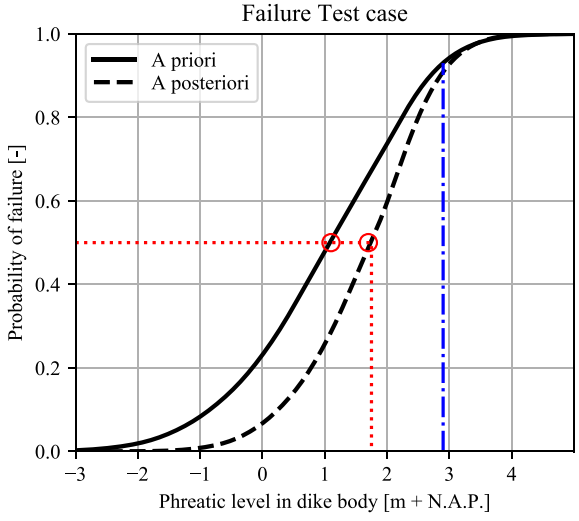

Fig. 10. Prior and posterior fragility curves of the failure test. The cumulative density curve does not show a sharp cut-off at the survived phreatic level during construction, but a gradual reduction of probability density at low phreatic levels, and a redistribution of density mass over the higher phreatic levels, due to the differences in loading conditions between the failure test and the survived construction.

presented in this paper. Therefore, the proposed approach is a convenient, practical alternative for estimating low probabilities. The use of surrogate-models for slope stability calculations (e.g., Jiang, Li, Cao, Zhou, & Phoon, 2015; Li, Zheng, Cao, Tang, & Phoon, 2016) may allow evaluation of Bayes' rule (Eq. (6)) directly, improving computational efficiency while using less approximations.

To assess whether incorporating construction survival can improve the reliability estimate in practical projects, we recommend analyzing first how critical were the loading conditions during construction, compared to the design loading conditions, in terms of the respective factors of safety. Yet, survival of a critical loading condition does not always result in a significant increase in reliability, since there are other influencing factors. For example, the correlation (i.e. the degree of similarity) between the assessed and survived situation has a major influence. Also the availability of information about, and hence, the uncertainty in the survived conditions plays a role in this. Therefore, we recommend to further investigate for example the contribution of unsaturated conditions to the shear strength, which was neglected in the examples.

The results also indicate that dikes on soft soil blankets that survived the construction will generally have a higher reliability than they were designed for. This knowledge could be used to optimize designs by anticipating the survival of the construction stage using pre-posterior analysis. The criticality of the loading condition during construction, the required monitoring (e.g. pore water pressures), and contingency actions (e.g. stopping criterion) become then elements in the optimization. Bayesian decision theory (Raiffa & Schlaifer, 1961) and the Observational Method (Spross & Johansson, 2017) provides an appropriate risk-based framework to consider whether the expected benefits in the design outweigh the additional risk of failure during construction.

To conclude, if construction survival is included in safety assessments of dikes, reliability estimates are expected to increase. This improves safety assessments of existing dikes and new dikes significantly. Since many dikes (at least in deltaic areas such as in the Netherlands) are built on clay or soft soil blankets, this will allow for more targeted and cost-effective investments in flood protection.

Data availability statement

Some or all data, models, or code that support the findings of this study are available from the corresponding author upon reasonable request.

Notation

d = model uncertainty factor
g = limit state function
m = strength increase exponent
s_u = spatially-averaged undrained shear strength
u_i = random number in the i^{th} Monte Carlo realization
u_i = random number in the i^{th} Monte Carlo realization
F = failure event
F_S = factor of safety
P = probability
S = normally consolidated undrained shear strength ratio
OCR = over-consolidation ratio
POP = pre-overburden pressure
$\mathbf{X}$ = vectors of stochastic variables
α_k = FORM influence factor for parameter k
β = reliability index
γ = volumetric weight
ε = evidence/survived event
φ_{cs} = critical state friction angle
μ = mean value
ρ = correlation coefficient
σ = standard deviation
σ'_v = effective vertical stress

σ'_p = preconsolidation stress
$\chi_{F,i}$ = indicator value of failure in the i^{th} Monte Carlo realization
$\chi_{\varepsilon,i}$ = indicator value of evidence in the i^{th} Monte Carlo realization

Declaration of Competing Interest

None.

Acknowledgements

This work is part of the research programme All-Risk with project number P15-21, which is (partly) financed by NWO Domain Applied and Engineering Sciences. The authors would like to thank the POVM, established in 2015 by Water Authorities in the Netherlands, who initiated and financed the 'Eemdijkproef'.

References

Azzouz, A.S., Baligh, M.M., Ladd, C.C., 1983. Corrected field vane strength for embankment design. J. Geotech. Eng. 109 (5), 730–734. https://doi.org/10.1061/(asce)0733-9410(1983)109:5(730).
Babu, G.L.S., Murthy, D.S., 2005. Reliability analysis of unsaturated soil slopes. J. Geotech. Geoenviron. 131 (11), 1423–1428. https://doi.org/10.1061/(ASCE)1090-0241(2005)131:11(1423).
Baecher, G.B., Christan, J.T., 2003. Reliability and Statistics in Geotechnical Engineering. Wiley, Chichester, U.K.
Baecher, G.B., Ladd, C.C., 1997. Formal observational approach to staged loading. Transport. Res. Rec. J. Transport. Res. Board 1582 (1), 49–52. https://doi.org/10.3141/1582-08.
Berre, T., Bjerrum, L., 1975. Shear strength of normally consolidated clays. In: Proc., 8th International Conference on Soil Mechanics and Foundation Engineering, 1, pp. 39–49. https://doi.org/10.1016/0148-9062(75)92250-0.
Bishop, A.W., 1955. The use of the slip circle in the stability analysis of earth slopes. Geotechnique 5, 7–17. https://doi.org/10.1680/geot.1955.5.1.7.
Cao, Z., Wang, Y., Li, D.Q., 2017. Probabilistic Approaches for Geotechnical Site Characterization and Slope Stability Analysis. Springer, Berlin. https://doi.org/10.1007/978-3-662-52914-0.
Ching, J., Phoon, K.K., Hu, Y.G., 2009. Efficient evaluation of reliability for slopes with circular slip surfaces using importance sampling. J. Geotech. Geoenviron. 135 (6), 768–777. https://doi.org/10.1061/(ASCE)GT.1943-5606.0000035.
Christian, J.T., Ladd, C.C., Baecher, G.B., 1994. Reliability applied to slope stability analysis. J. Geotech. Eng. 120 (12), 2180–2207. https://doi.org/10.1061/(asce)0733-9410(1996)122:5(417).
De Koker, N., Day, P., Zwiers, A., 2018. Assessment of reliability-based design of stable slopes. Can. Geotech. J. 56 (4), 495–504. https://doi.org/10.1139/cgj-2018-0149.
De Koning, M., Simanjuntak, T.D.Y.F., Goeman, D.G., Bakker, H.L., Haasnoot, J.K., Bisschop, C., 2019. Determination of SHANSEP parameters by laboratory tests and CPTu for probabilistic model-based safety analyses. In: Proceedings of the XVII European Conference on Soil Mechanics and Geotechnical Engineering 2019. https://doi.org/10.32075/17ECSMGE-2019-0073.
Deltares, 2015. Modelonzekerheidsfactoren Spencer-Van der Meij model en ongedraineerde schuifsterkte. Deltares report 1207808-001 (in Dutch). Retrieved from. http://publications.deltares.nl/1207808_001.pdf.
Deltares, 2018a. Project software macro stability. User manual 2018, Part 3: Scientific Background. Deltares Report 11201523. https://www.deltares.nl/app/uploads/2019/06/4.-MacroStability-Kernel-Scientific-Manual-Exclude-Manual.pdf.
Deltares, 2018b. POVM Eemdijkproef. Geotechnisch Basisrapport. Product F. Deltares report 11200956-002-GEO-0015 (in Dutch). Retrieved from: https://publicwiki.deltares.nl/display/POVM/Achtergronddocumenten+en+Software#AchtergronddocumentenenSoftware-Praktijkproeven-Damwand.
Deltares, 2018c. POVM Eemdijkproef. Factual report monitoring aanleg full-scaleproeven. Product R. Deltares report 11200956-000-GEO-0003 (in Dutch). Retrieved from: https://publicwiki.deltares.nl/display/POVM/Achtergronddocumenten+en+Software#AchtergronddocumentenenSoftware-Praktijkproeven-Damwand.
Feijten, E., 2018, March 9. De ringdijk bij Eemnes vanuit de lucht. Retrieved from. https://nos.nl/artikel/2222965-met-damwand-versterkte-proefdijk-zakt-na-acht-dagen-in.html.
Griffiths, D.V., Huang, J., Fenton, G.A., 2009. Influence of spatial variability on slope reliability using 2-D random fields. J. Geotech. Geoenviron. 135 (1), 1367–1378. https://doi.org/10.1061/(ASCE)GT.1943-5606.0000099.
Hasofer, A.M., Lind, N.C., 1974. Exact and invariant second-moment code format. J .Eng. Mech. Div. 100 (1), 111–121.
Huber, M., M. G. van der Krogt, and W. Kanning. 2016. "Probabilistic slope stability analysis using approximative FORM." Proc., 14th International Probabilistic Workshop, Springer International Publishing, 299–316. Doi:https://doi.org/10.1007/978-3-319-47886-9_21.
Jiang, S.H., Huang, J., Qi, X.H., Zhou, C.B., 2020. Efficient probabilistic back analysis of spatially varying soil parameters for slope reliability assessment. Eng. Geol. 271, 105597 https://doi.org/10.1016/j.enggeo.2020.105597.
Jiang, S.H., Li, D.Q., Cao, Z.J., Zhou, C.B., Phoon, K.K., 2015. Efficient system reliability analysis of slope stability in spatially variable soils using Monte Carlo simulation. ASCE J. Geotech. Geoenviron. Eng. 141 (2) (04014096).
Jonkman, S.N., Voortman, H.G., Klerk, W.J., van Vuren, S., 2018. Developments in the management of flood defences and hydraulic infrastructure in the Netherlands. Struct. Infrastruct. Eng. 14 (7), 895–910. https://doi.org/10.1080/15732479.2018.1441317.
Juang, C.H., Gong, W., Martin, J.R., Chen, Q., 2018. Model selection in geological and geotechnical engineering in the face of uncertainty - does a complex model always outperform a simple model? Eng. Geol. 184–196. https://doi.org/10.1016/j.enggeo.2018.05.022.
Juang, C.H., Zhang, J., Shen, M., Hu, J., 2019. Probabilistic methods for unified treatment of geotechnical and geological uncertainties in a geotechnical analysis. Eng. Geol. 249, 148–161. https://doi.org/10.1016/j.enggeo.2018.12.010.
Kanning, W., Teixeira, A., van der Krogt, M.G., Rippi, K., Schweckendiek, T., Hardeman, B., 2017. Calibration of factors of safety for slope stability of dikes. In: Proc. Geo-Risk 2017, American Society of Civil Engineers, pp. 1–10. https://doi.org/10.1061/9780784480717.001.
Ladd, C.C., 1991. Stability Evaluation during Staged Construction. J. Geotech. Eng. 117 (4), 540–615.
Ladd, C.C., Degroot, D.J., 2003. Recommended Practice for Soft Ground Site Characterization. In: Proc., 12th Panamerican Conference on Soil Mechanics and Geotechnical Engineering. United States of America, Cambridge, pp. 1–55.
Ladd, C.C., Foott, R., 1974. Design procedure for stability of soft clay. J. Geotech. Eng. Div. 100 (7), 763–786.
Lengkeek, H.J., Post, M., Breedeveld, J., Naves, T., 2019. Eemdijk full-scale field test programme: ground dyke and sheet pile dyke failure test. In: Proc., XVII European Conference on Soil Mechanics and Geotechnical Engineering, Iceland, Reykjavik. https://doi.org/10.32075/17ECSMGE-2019-0454.
Li, D.Q., Zhang, F.P., Cao, Z.J., Zhou, W., Phoon, K.K., Zhou, C.B., 2015. Efficient reliability updating of slope stability by reweighting failure samples generated by Monte Carlo simulation. Comput. Geotech. 69, 588–600. https://doi.org/10.1016/j.compgeo.2015.06.017.
Li, D.Q., Zheng, D., Cao, Z.J., Tang, X.S., Phoon, K.K., 2016. Response surface methods for slope reliability analysis: Review and comparison. Eng. Geol. 203, 3–14. https://doi.org/10.1016/j.enggeo.2015.09.003.
Ochiai, H., 1980. Undrained Strength of Normally Consolidated Clay Measured in the Simple Shear Test, 15. Nagasaki University Research Report, pp. 73–78.
Phoon, K.K., Kulhawy, F.H., 1999a. Characterization of geotechnical variability. Can. Geotech. J. 36 (4), 612–624. https://doi.org/10.1139/t99-038.
Phoon, K.K., Kulhawy, F.H., 1999b. Evaluation of Geotechnical Property Variability. Can. Geotech. J. 36 (4), 625–639. https://doi.org/10.1139/t99-039.
Raiffa, H., Schlaifer, R., 1961. Applied Statistical Decision Theory. Division of Research, Harvard Business School, Boston, MA.
Roscoe, K., Diermanse, F., Vrouwenvelder, T., 2015. System reliability with correlated components: Accuracy of the Equivalent Planes method. Struct. Saf. 57, 53–64. https://doi.org/10.1016/j.strusafe.2015.07.006.
Schofield, A., Wroth, P., 1968. Critical State Soil Mechanics. McGraw Hill, Maidenhead.
Schweckendiek, T., 2010. In: Reassessing Reliability Based on Survived Loads. Proc. International Conference of Coastal Engineering. Texas Digital Library, Shanghai, pp. 1–14.
Schweckendiek, T., van der Krogt, M.G., Teixeira, A., Kanning, W., Brinkman, R., Rippi, K., 2017. Reliability updating with survival information for dike slope stability using fragility curves. In: Proc. Geo-Risk, vol. 2017. United States of America, Denver, pp. 494–503.
Schweckendiek, T., Vrouwenvelder, A.C.W.M., Calle, E.O.F., 2014. Updating piping reliability with field performance observations. Struct. Saf. 47, 13–23. https://doi.org/10.1016/j.strusafe.2013.10.002.
Schweckendiek, T., Vrouwenvelder, A.C.W.M., Calle, E.O.F., Kanning, W., Jongejan, R. B., 2013. Target reliabilities and partial factors for flood defenses in the Netherlands. In: Proc., Modern Geotechnical Design Codes of Practice. IOS Press, Lansdale, pp. 311–328. https://doi.org/10.3233/978-1-61499-163-2-311.
Shewbridge, S., Schaefer, J., 2013. Some unexpected 'modern' complications in seepage and slope stability analysis: Modeling pore pressures and strengths for flood-loaded structures. In: Proc. Annual Conference, Association of State Dam Safety Officials, pp. 694–714.
Spross, J., Johansson, F., 2017. When is the observational method in geotechnical engineering favourable? Struct. Saf. 66, 17–26. https://doi.org/10.1016/j.strusafe.2017.01.006.
Straub, D., Papaioannou, I., 2014. Bayesian analysis for learning and updating geotechnical parameters and models with measurements. In: Phoon, K.K., Ching, J.Y. (Eds.), Chapter 5 in Risk and Reliability in Geotechnical Engineering. CRC Press, Boca Raton, FL, pp. 221–264.
Stuedlein, A.W., Kramer, S.L., Arduino, P., Holtz, R.D., 2012. Geotechnical Characterization and Random Field Modeling of Desiccated Clay. J. Geotech. Geoenviron. 138 (11), 1301–1313. https://doi.org/10.1061/(ASCE)GT.1943-5606.0000723.
Tavenas, F., Mieussens, C., Bourges, F., 1979. Lateral displacements in clay foundations under embankments. Can. Geotech. J. 16 (3), 532–550. https://doi.org/10.1139/t79-059.
U.S. Army Corps of Engineers. (USACE), 2003. EM 1110–2-1902, Engineering Manual, Engineering and Design, Slope Stability.
Van, M., 2001. New approach for uplift induced slope failure. In: Proc. XVth International Conference on Soil Mechanics and Geotechnical Engineering, Istanbul, pp. 2285–2288.

Van der Krogt, M.G., Schweckendiek, T., 2019. Systematic transformation error in the depth-average undrained shear strength. In: Proc. 7th International Symposium on Geotechnical Safety and Risk (ISGSR 2019), Taipei, Taiwan, pp. 11–13.

Van der Krogt, M.G., Schweckendiek, T., Kok, M., 2018. Uncertainty in spatial average undrained shear strength with a site-specific transformation model. Georisk: Assess. Manage. Risk Eng. Syst. Geohazards 13 (3), 226–236. https://doi.org/10.1080/17499518.2018.1554820.

Vanmarcke, E.H., 1980. Probabilistic Stability Analysis of earth slopes. Eng. Geol. 16, 29–50. https://doi.org/10.1016/0013-7952(80)90005-8.

Watabe, Y., Tsuchida, T., Adachi, K., 2002. Undrained shear strength of pleistocene clay in Osaka Bay. J. Geotech. Geoenviron. 128 (3), 216–226. https://doi.org/10.1061/(ASCE)1090-0241(2002)128:3(216).

Zhang, L.L., Zhang, L.M., Tang, W.H., 2005. Rainfall-induced slope failure considering variability of soil properties. Geotechnique 55 (2), 183–188. https://doi.org/10.1680/geot.2005.55.2.183.

Zhang, J., Zhang, L.M., Tang, W.H., 2011. Slope reliability analysis considering site-specific performance information. J. Geotech. Geoenviron. 137 (3), 227–238. https://doi.org/10.1061/(ASCE)GT.1943-5606.0000422.